

## Chapter 4

### Conclusions and Recommendations for Future Work

#### 4.1 Conclusions

X-ray absorption fine structure (XAFS) was used to characterize a series of silica-supported manganese oxide catalysts of loadings ranging from 3 to 20 wt. %. At the lowest loading (3 wt. %), manganese oxide was atomically dispersed, but with increased loading (10 – 20 wt. %), the oxidation state and structure of the catalysts resembled first  $\text{Mn}_2\text{O}_3$  and then  $\text{Mn}_3\text{O}_4$ . Specifically, as metal oxide loading was increased, the absorption energies and Mn-O coordination numbers decreased while the Mn-O bond distances increased from values characteristic of bulk  $\text{Mn}_2\text{O}_3$  to values typical of  $\text{Mn}_3\text{O}_4$ . The white line areas calculated for the catalyst series confirmed that the oxidation state of the Mn decreased with increasing loading. The white line regions in the XANES spectra for the catalyst series were compared to those of the bulk reference compounds  $\text{MnO}$ ,  $\text{Mn}_3\text{O}_4$ ,  $\text{Mn}_2\text{O}_3$ , and  $\text{MnO}_2$ . The shape of the white line region for the supported catalysts, along with the fine structure located beyond the white line, was most similar to that of  $\text{Mn}_3\text{O}_4$ . XRD supported the assignment of  $\text{Mn}_3\text{O}_4$  being the main manganese oxide phase found in the high loading samples.

Laser Raman spectroscopy experiments showed two adsorbates on the surface of the 10 wt. %  $\text{MnO}_x/\text{SiO}_2$  catalyst during the reaction of acetone and ozone. The peak

associated with ozone was located at  $890\text{ cm}^{-1}$  and was identified as a peroxide species (O-O band). The peak associated with the acetone was located at  $2930\text{ cm}^{-1}$  and was attributed to a C-H stretching mode.

Reactivity studies performed on the 3 wt. % and 10 wt. %  $\text{MnO}_x/\text{SiO}_2$  showed that the 10 wt. % catalyst gave higher rates for both acetone and ozone conversion compared to the 3 wt. % catalyst. Studies comparing ozone and oxygen as the oxidant for the reaction showed that the use of ozone yielded higher acetone conversion at lower temperatures. The use of ozone as the oxidant significantly reduced the activation energy for the reaction at low temperatures compared to when oxygen was used, and indicated the opening of a new reaction pathway. Studies that compared the presence and absence of acetone with ozone showed that rates of ozone conversion were higher when acetone was absent from the reaction. Since acetone and ozone species were competing for sites on the catalyst surface, the absence of acetone allowed the ozone to react with more sites, thus increasing the rate of ozone conversion.

The higher loading catalysts had higher turnover rates for the oxidation of acetone. This could be due to the site requirements for the addition of multiple oxygen atoms to the adsorbed acetone intermediate. It could also be associated with the greater ease of electron acceptance by the manganese oxide center in the rate-determining step of acetone oxidation.

The steady-state and transient kinetics of the oxidation of acetone using ozone over a silica-supported manganese oxide catalyst was studied using acetone partial pressures from 101 – 405 Pa, ozone partial pressure from 101 – 1013 Pa, and temperatures of 318, 333, 343, and 373 K. Raman spectroscopy experiments identified

an adsorbed acetone species at  $2930\text{ cm}^{-1}$  on the silica support and an adsorbed peroxide species due to ozone at  $890\text{ cm}^{-1}$  on the manganese oxide. The steady-state kinetics for the acetone and ozone reactions were found to be reasonably described by both a power rate law model and a Langmuir-Hinshelwood model. Transient experiments, conducted for both acetone and ozone, were used to separately measure the rate of reactant adsorption and the rate of reactant removal (desorption plus reaction) to and from the catalyst surface. By setting the rate of adsorption equal to the rate of removal, steady-state rates for both acetone and ozone reaction as well as coverages for both the acetone and peroxide intermediates were calculated. The coverages obtained through transient experiments compared favorably to those obtained from *in situ* Raman spectroscopy measurements under steady-state conditions. However, only the steady-state rate of acetone reaction obtained through the transient experiments compared favorably to the results obtained under steady-state conditions. Thus, the role of the adsorbed acetone intermediate was determined to be described by the proposed reaction mechanism while the adsorbed peroxide species was determined to be a spectator in the acetone oxidation reaction. The mechanism was proposed to involve a dual site reaction between an adsorbed acetone species and an adsorbed atomic oxygen species to form complete oxidation products.

## 4.2 Recommendations For Future Work

### 4.2.1 *Ab Initio* Calculations

*Ab initio* molecular orbital calculations using the Gaussian 98 software could be conducted to aid in the determination of the catalyst structure along with the structure of acetone adsorbed on the surface of the catalyst. This would be done by comparing the calculated results with experimental ones. For example, bond lengths determined by EXAFS analysis and vibrational frequencies determined by Raman spectroscopy could be compared to calculated values. By comparing several calculated structures to the experimental results, final geometries could be obtained. The total energies found from these optimized geometries could also be used to calculate the heats of formation ( $\Delta H_f$ ), which could help determine if the process of adsorption is energetically favorable.

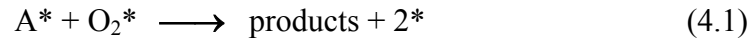
### 4.2.2 Non-Uniform Surface Kinetic Analysis

In the present work, it was concluded through Raman spectroscopy and temperature programmed desorption (TPD) measurements that acetone adsorbed mainly to the silica support while a peroxide intermediate attributed to ozone adsorbed to the manganese. It was also concluded based on a transient kinetic study that the adsorbed peroxide intermediate was a spectator species and did not contribute to the oxidation of acetone. It was then proposed that an atomically adsorbed oxygen intermediate was directly involved in the acetone reaction. The steady-state kinetics for the catalytic oxidation of acetone using ozone fit equally well to a power rate law and a Langmuir-

Hinshelwood expression. Therefore, it was not determined through the present analysis whether the catalyst surface was uniform or non-uniform in nature.

There have been many studies that have reported kinetically heterogeneous surfaces due to lateral interactions between adsorbates [1,2] and the presence of a distribution of sites [3,4,5]. Also, non-uniform surfaces were reported for work done on ozone decomposition on  $\text{MnO}_x/\text{Al}_2\text{O}_3$  [6,7] and ethanol oxidation on  $\text{MoO}_3/\text{SiO}_2$  [8]. In these studies, reaction rates varied exponentially with adsorbate coverage, and therefore, could not be described by a Langmuir-Hinshelwood expression, which assumes a uniform surface. The same type of analysis could be performed for the case of acetone oxidation with ozone, but in this case, however, two adsorbates would need to be considered. This non-uniform surface kinetic analysis could verify that the adsorbed peroxide species attributed to ozone does not contribute to the reaction and could also provide a deeper understanding of the catalyst surface.

It is important to note that for this analysis, it would be assumed that the final step of the mechanism would involve the reaction between the adsorbed acetone intermediate and peroxide species as shown below since the peroxide species is the only observable oxygen species in the Raman spectroscopy measurements:



If the activations energies were assumed to vary linearly with coverage [9], then the activation energy for the reaction shown in Eq. 4.1 would be given by

$$E = E^o - RTh\theta_A - RTh'\theta_{\text{O}_2^*}, \quad (4.2)$$

where  $h$  and  $h'$  are parameters that describe the non-uniformity and  $^o$  denotes the empty surface. The rate of the reaction could then be derived to be

$$r = k^o \exp(h\theta_A) \exp(h'\theta_{O_2^*}) \quad (4.3)$$

$$r = k^o \left[ \frac{k_A^o}{k_{-A}^o} (A) \right]^{f+g} \left[ \frac{k_{O_2^*}^o}{k_{-O_2^*}^o} (O_3) \right]^{f'+g'} \quad (4.4)$$

where the  $k$ 's are rate constants for the adsorption and desorption steps involving acetone and ozone, and the  $f$ 's,  $g$ 's, and  $h$ 's are again non-uniform surface parameters. Even though the above rate expression (Eq. 4.4) looks very complex, it is possible to determine the values of all unknowns by simultaneously fitting rate and coverage data. This method has been used for one adsorbate [10] in an ozone decomposition study and should be possible for two adsorbates considering data is available in which one reactant is varied while the other is constant and vice versa.

The success or failure of this method would aid in verifying the mechanism proposed in this study as well as the roles of the adsorbed intermediates. It should also provide a deeper understanding of the nature of active sites found in the catalyst.

### 4.2.3 Loading and Support Effects

In the present work, it was found that the structure for the 3 wt. %  $MnO_x/SiO_2$  catalyst was quite different than that for the 10, 15, and 20 wt. %  $MnO_x/SiO_2$  catalysts. The EXAFS analysis of the 3 wt. %  $MnO_x/SiO_2$  sample showed that the coordination around each Mn atom was composed of 6 Mn-O distances and no appreciable Mn-Mn contribution, indicating that the Mn clusters were essentially atomically dispersed and had an octahedral structure. The XANES spectra suggested an oxidation state close to  $Mn_2O_3$  (+3). The EXAFS analysis of the 10, 15, and 20 wt. %  $MnO_x/SiO_2$  samples indicated that they had Mn-O and Mn-Mn distances consistent with  $Mn_3O_4$ , and the

XANES spectra also suggested an oxidation state close to  $\text{Mn}_3\text{O}_4$  ( $+2\frac{2}{3}$ ). The white line analysis of the XANES data supported the trend that the Mn oxidation state decreased with increased loading.

Even though there is confidence in the characterization of the catalysts used in this study, it could be of interest to look at other loadings for the  $\text{MnO}_x/\text{SiO}_2$  catalyst. For the catalyst studied in this work, there is a definite difference between the 3 wt. %  $\text{MnO}_x/\text{SiO}_2$  catalyst and the 10, 15, 20 wt. %  $\text{MnO}_x/\text{SiO}_2$  catalysts. Above 10 wt. %, increased loading resulted in the same active manganese oxide phase. It would be interesting to also characterize catalysts of possibly 1 and 6 wt. % to more fully understand the effect of loading on the active manganese oxide phase. Characterization of a 1 wt. %  $\text{MnO}_x/\text{SiO}_2$  catalyst could possibly result in a higher manganese oxidation state such as in  $\text{MnO}_2$ . Characterization of a 6 wt. %  $\text{MnO}_x/\text{SiO}_2$  catalyst could give more information of the transition from  $\text{Mn}_2\text{O}_3$  (3 wt. %  $\text{MnO}_x/\text{SiO}_2$ ) to  $\text{Mn}_3\text{O}_4$  (10 wt. %  $\text{MnO}_x/\text{SiO}_2$ ).

It would also be of interest to study the catalytic oxidation of acetone using ozone over manganese oxide for catalysts with different supports. Support effects are often present in oxidation reactions where electron transfer is important. Thus, it is probable that the support would affect the reactivity of manganese oxide for the reaction between acetone and ozone. It has been reported that the effect of the support on catalyst activity is large for both ozone decomposition on manganese oxide [7,10] and methanol oxidation on vanadium oxide [11,12]. For example, turnover rates increased by three orders of magnitude with support in the case of methanol oxidation on vanadium oxide in the order

$\text{SiO}_2 < \text{Al}_2\text{O}_3 < \text{TiO}_2 < \text{ZrO}_2 < \text{CeO}_2$ . Therefore, the effect of support would be an interesting subject of future study to determine the process of electron transfer.

## References

- 1 R. J. Madix, Selected principles in surface reactivity: reaction kinetics on extended surfaces and the effects of reaction on surface reactivity, "The Chemical Physics of Solid Surfaces and Heterogeneous Catalysis," Vol. 4, Elsevier: New York, 1983, 1.
- 2 S. J. Lombardo, A. T. Bell, A review of theoretical models for adsorption, diffusion, desorption, and reaction of gases on metals, *Surf. Sci. Rep.*, **1991**, 13, 1.
- 3 L. E. Razon, R. A. Schmitz, Multiple and instabilities in chemically reacting systems – a review, *Chem. Eng. Sci.*, **1987**, 42, 1005.
- 4 C. G. Takoudis, L. D. Schmidt, R. Aris, Steady-state multiplicity in surface reactions with coverage dependent parameters, *Chem. Eng. Sci.*, **1981**, 36, 1795.
- 5 M. Boudart, Heterogeneity of metal surfaces, *J. Am. Chem. Soc.*, **1952**, 74, 3556.
- 6 W. Li, G. V. Gibbs, S. T. Oyama, Mechanism of ozone decomposition on manganese oxide: 1. in situ laser Raman spectroscopy and ab initio molecular orbital calculations, *J. Am. Chem. Soc.*, **1998**, 120, 9041.
- 7 W. Li., S. T. Oyama, The mechanism of ozone decomposition on manganese oxide: 2. steady-state and transient kinetic studies, *J. Am. Chem. Soc.*, **1998**, 120, 9047.
- 8 W. Zhang, S. T. Oyama, In situ laser Raman studies of intermediates in the catalytic oxidation of ethanol, *J. Phys. Chem.*, **1996**, 100, 10759.
- 9 S. Brunauer, K. S. Love, R. G. Keenan, Adsorption of nitrogen and the mechanism of ammonia decomposition over iron catalysts, *J. Am. Chem. Soc.*, **1942**, 64, 751.
- 10 R. Radhakrishnan, S. T. Oyama, Ozone decomposition over manganese oxide supported on ZrO<sub>2</sub> and TiO<sub>2</sub>: a kinetic study using in situ laser Raman spectroscopy, *J. Catal.*, **2001**, 199, 282.

- 11 G. Deo, I. E. Wachs, Reactivity of supported vanadium oxide catalysts: the partial oxidation of methanol, *J. Catal.*, **1994**, 146, 323.
- 12 I. E. Wachs, G. Deo, M. A. Vuurman, H. Hu, D. S. Kim, J. M. Jehng, Molecular design of supported metal oxide catalysts: an initial step to theoretical models, *J. Mol. Catal.*, **1993**, 82, 443.